AIAA AVIATION Forum
12-16 June 2023, San Diego, CA and Online
AIAA AVIATION 2023 Forum

10.2514/6.2023-4436

Study of 3D Flapped CoFlow Jet Wings for Ultra-High Cruise Lift Coefficient

Jaehyoung Jeon * Brendon McBreen † Yan Ren ‡ Gecheng Zha §
Dept. of Mechanical and Aerospace Engineering
University of Miami, Coral Gables, Florida 33124
E-mail: gzha@miami.edu

Abstract

The previous research indicates a possibility of increasing subsonic 2D airfoil cruise lift coefficient C_L by an order of magnitude from 0.4 to 4 with a flapped coflow jet airfoil modified from CFJ-NACA-6421 airfoil at a reasonable aerodynamic efficiency of 48. This paper is to extend the study to 3D wings formed by the same airfoil at various aspect ratios to understand the performance penalized by induced drag. A high cruise lift coefficient is important for ultra-high altitude flight on Earth and flight in Martian atmosphere to overcome the low atmospheric density. The research is based on validated CFD simulation, which employs a 3D RANS solver with Spalart-Allmaras(SA) turbulence model, a fifth-order WENO scheme for the inviscid fluxes, second-order central differencing for the viscous terms. As a validation, the numerical simulation achieves a very good agreement with the experiment for a 3D wing formed by NACA6421 airfoil with an aspect ratio of 6. The study investigates the 3D CFJ flapped wing at aspect ratio(AR) of 6, 10 and 20 at a freestream Mach number of 0.17 and Reynolds number of 3.48×10^6. For the one with AR of 20, a C_L of 3.76 and a moderate $(C_L/C_D)_c$ of 10.55 are obtained. This research indicates that cruise flight at an ultra-high lift coefficient with an acceptable aerodynamic efficiency appears to be feasible.

Nomenclature

CFJ	CoFlow jet
$FCFJ$	Flapped CoFlow jet
$AoA(\alpha)$	Angle of attack
AR	Aspect Ratio
β	Deflection angle
LE	Leading Edge
TE	Trailing Edge
s	Wing Span length
c	Profile chord

* Ph.D. Student
† Ph.D. Candidate
‡ Postdoc Researcher, Ph.D., AIAA member
§ Professor, ASME Fellow, AIAA associate Fellow

U	Flow velocity
q	Dynamic pressure $0.5\,\rho\,U^2$
p	Static pressure
ρ	Air density
$\dot{m}$	Mass flow
M	Mach number
ω	Pitching Moment
P	Pumping power
∞	Free stream conditions
C_L	Lift coefficient $L/(q_\infty\,S)$
C_D	Drag coefficient $D/(q_\infty\,S)$
C_μ	Jet momentum coef. $\dot{m}_j\,U_j/(q_\infty\,S)$
Pc	Power coefficient $L/(q_\infty\,S\,V_\infty)$
$(C_L/C_D)_c$	CFJ airfoil corrected efficiency $L/(D\,P/V_\infty)$
R_e	Reynolds number
M	Mach number
c_p	Constant pressure specific heat
γ	Air specific heats ratio
S	Planform area of the wing
ρ_∞	Density
V_∞	Velocity
T_t	Total temperature
P_t	Total pressure
H_t	Total specific enthalpy
$\dot{m}$	Mass flow across the pump
$_\infty$	Subscript, stands for free stream
$_j$	Subscript, stands for jet

1 Introduction

The most important phase of an aircraft's flight envelope is typically the cruise flight to achieve high mission effectiveness, long range, and high transportation capacity (i.e., *payload* $\times$ *range*). An aircraft at cruise must fly with a high aerodynamic efficiency C_L/C_D while maintaining a sufficient stall margin. In order to have high aerodynamic efficiency, a typical subsonic wing adopts a thickness of around 15% and provides a cruise lift coefficient of 0.4 to 0.6. A 20% or thicker airfoil could have a greater cruise lift coefficient. However, the thick airfoil is rarely employed since it is prone to flow separation and stall. The takeoff and landing phase of aircraft requires a high lift coefficient, particularly if a short takeoff and landing distance is desired. With multi-element flaps, conventional high-lift wings can get a maximum lift coefficient of around 2.5. No aircraft would, however, cruise at such a high lift coefficient since the aircraft would be near stall and the very large drag coefficient would make most of the missions unfeasible.

However, there are situations that an ultra-high cruise lift coefficient is desirable provided an acceptable aerodynamic efficiency can be achieved. For example, it is very beneficial to have an extraordinarily high cruise lift coefficient in order to fly on Mars. It is needed to overcome the low density of the Martian atmosphere and maintain a compact size and light weight of the aircraft. Similar situation exists to fly at ultra-high altitude such

as at 30,000 m in Earth's atmosphere. Using active flow control (AFC) makes an ultra-high cruise lift coefficient possible. However, it is challenging to use AFC for cruise because the advantages may not outweigh the costs of AFC energy, preventing a net efficiency improvement for the entire aircraft system.

The CoFlow Jet (CFJ) flow control airfoil is a promising AFC with the potential to improve cruise efficiency[1, 2, 3, 4, 5, 6, 7, 8, 9, 10, 11, 12, 13, 14, 15, 16]. Fig. 1 depicts a regular CFJ airfoil compared with the baseline airfoil. A small mass flow is sucked into the suction duct, compressed, and energized by a pump before being injected tangentially into the main flow near the leading edge. The studies of Lefebvre et al [8, 17] and Wang and Zha [18] indicate that 2D CFJ airfoils could reach a noticeably better cruise lift coefficient and aerodynamic efficiency, which is defined as

$$(\frac{C_L}{C_D})_c = \frac{C_L}{C_D + P_c} \tag{1}$$

where Pc is the CFJ required power coefficient. However, for 3D wings with finite aspect ratios, the CFJ wings can still maintain high cruise C_L, but the aerodynamic efficiency is decreased to the level of its baseline counterparts [19]. To reflect the transportation productivity of aircraft represented by the range multiplied by the gross weight, a cruise productivity efficiency is introduced as [12]:

$$(\frac{C_L^2}{C_D})_c = \frac{C_L^2}{(C_D + Pc)} \tag{2}$$

CFJ wing can have substantially higher cruise C_L and thus greater productivity efficiency as well than conventional wings with no flow control. Taking advantage of the CFJ wing high cruise lift coefficient and thus high suction effect on wing upper surface, Ren and Zha [20] design a tandem wing aircraft configuration that the front wing tip vortex is captured by the rear wing to enhance the overall system efficiency. With an aspect ratio of 9, the numerically simulated tandem air vehicle achieves a cruise C_L of 1.6 and $(C_L/C_D)_c$ of 13. The cruise C_L of 1.6 is beyond the reach of conventional design, which would be either stalled or suffer very high drag increase and poor aerodynamic efficiency. This paper is motivated to push even further the cruise lift coeffecient.

CFJ airfoil can achieve very high maximum lift coefficient exceeding the theoretical limit of $C_{Lmax} = 2\pi(1+t/c)$ up to 13 and beyond [12, 13, 19, 21]. However, for cruise condition, the regular CFJ configuration as shown in Fig. 1 appears to have rapid energy consumption increase when C_L is greater than 1.6[12, 22]. Even though the aerodynamic drag coefficient C_D can remain small and the pure aerodynamic lift to drag ratio C_L/C_D can be still very high, the corrected aerodynamic efficiency defined in Eq. (1) can decrease quickly with the increasing C_L when it is greater than 1.6.

To push cruise lift coefficient higher to the level of 4.0, Jeon et al [23] found the 2D airfoil with coflow jet applied on the flap is a promising candidate that can potentially maintain an acceptable aerodynamic efficiency of $(C_L/C_D)_c$. Such airfoil is named flapped CFJ airfoil that is originated form the deflected slipstream study for VTOL aircraft [24].

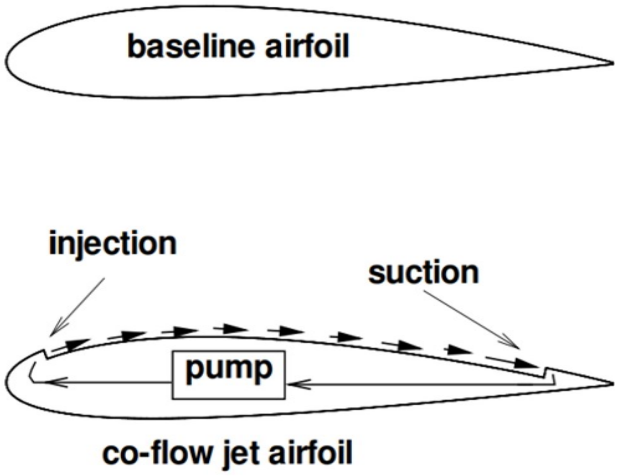

Figure 1: Sketch of CoFlow Jet airfoil

1.1 Flapped CoFlow Jet(FCFJ) Airfoil

The concept of flapped coflow jet airfoil is adopted from the CFJ airfoil with deflected slipstream for VTOL aircraft [24]. It is also guided by the CoFlow jet flow separation mechanism study of Xu and Zha [25].

The CFJ is applied inside a long flap that is a part of the flapped CFJ airfoil, as shown in Fig.2 [23], which has the injection located at the shoulder of the flap. The regular CFJ airfoil applies the injection very close to the leading edge at a point of around 2-4% Chord location. By deflecting the flap rather than rotating the front of the airfoil, the FCFJ airfoil has the advantage of allowing the airfoil to change the angle of attack and lift coefficient without tilting the wings or the aircraft. The goal of this work is to demonstrate numerically that the 3-dimensional FCFJ wing is a strong contender to achieve an ultra-high cruise lift coefficient satisfying a reasonable aerodynamic efficiency of $(C_L/C_D)_c$.

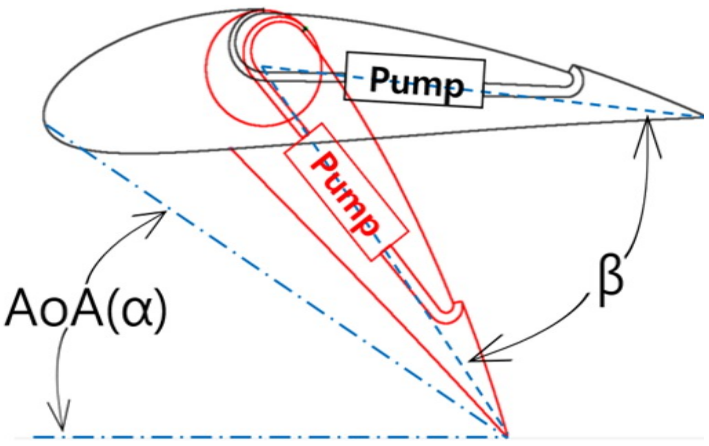

Figure 2: Sketch of flapped CFJ airfoil with the CoFlow jet applied on the flap

2 Methodology

2.1 Lift and Drag Calculation

The momentum and pressure at the injection and suction slots produce a reactionary force, which is automatically measured by the force balance in wind tunnel testing. However, for CFD simulation, the full reactionary force needs to be included. Using control volume analysis, the reactionary force can be calculated using the flow parameters at the injection and suction slot opening surfaces. Zha et al.[2] give the following formulations to calculate the lift and drag due to the jet reactionary force for a CFJ airfoil. By considering the effects of injection and suction jets on the CFJ airfoil, the expressions for these reactionary forces are given as :

$$F_{x_{cfj}} = (\dot{m}_j V_{j1} + p_{j1} A_{j1}) * cos(\theta_1 - \alpha) - (\dot{m}_j V_{j2} + p_{j2} A_{j2}) * cos(\theta_2 + \alpha) \tag{3}$$

$$F_{y_{cfj}} = (\dot{m}_{j1} V_{j1} + p_{j1} A_{j1}) * sin(\theta_1 - \alpha) + (\dot{m}_{j2} V_{j2} + p_{j2} A_{j2}) * sin(\theta_2 + \alpha) \tag{4}$$

where the subscripts 1 and 2 stand for the injection and suction respectively, and θ_1 and θ_2 are the angles between the injection and suction slot's surface and a line normal to the airfoil chord. α is the angle of attack.

The total lift and drag on the airfoil can then be expressed as:

$$D = R'_x - F_{x_{cfj}} \tag{5}$$

$$L = R'_y - F_{y_{cfj}} \tag{6}$$

where R'_x and R'_y are the surface integral of pressure and shear stress in x (drag) and y (lift) direction excluding the internal ducts of injection and suction. For CFJ wing simulations, the total lift and drag are calculated by integrating Eqs.(5) and (6) in the spanwise direction.

2.2 Jet Momentum Coefficient

The jet momentum coefficient C_μ is a parameter used to quantify the jet intensity. It is defined as:

$$C_\mu = \frac{\dot{m} V_j}{\frac{1}{2}\rho_\infty {V_\infty}^2 S} \tag{7}$$

where $\dot{m}$ is the injection mass flow, V_j is the mass-averaged injection velocity, ρ_∞ and V_∞ denote the free stream density and velocity, and S is the planform area.

2.3 Micro-compressor Power Coefficient

CFJ is implemented by mounting a pumping system inside the wing that withdraws air from the suction slot and blows it into the injection slot. The power consumption is determined by the jet mass flow and total enthalpy change as the following:

$$P = \dot{m}(H_{t1} - H_{t2}) \tag{8}$$

where H_{t1} and H_{t2} are the mass-averaged total enthalpy in the injection cavity and suction cavity respectively, P is the Power required by the pump and $\dot{m}$ the jet mass flow rate. Introducing P_{t1} and P_{t2} the mass-averaged total pressure in the injection and suction cavity respectively, the compressor efficiency η, and the total pressure ratio of the pump $\Gamma = \frac{P_{t1}}{P_{t2}}$, the power consumption is expressed as:

$$P = \frac{\dot{m} C_p T_{t2}}{\eta} (\Gamma^{\frac{\gamma-1}{\gamma}} - 1) \tag{9}$$

where γ is the specific heat ratio equal to 1.4 for air. The power coefficient is expressed as:

$$P_c = \frac{P}{\frac{1}{2}\rho_\infty V_\infty^3 S} \tag{10}$$

2.4 Aerodynamic Efficiency

The conventional wing aerodynamic efficiency is defined as:

$$\frac{C_L}{C_D} \tag{11}$$

For the CFJ wing, the ratio above still represents the pure aerodynamic relationship between lift coefficient and drag coefficient. However since CFJ active flow control consumes energy, the ratio above is modified to take into account the energy consumption of the micro-compressor. The formulation of the corrected aerodynamic efficiency for CFJ wings is the one defined in Eq.(1). If the micro-compressor power coefficient is set to 0, this formulation returns to the aerodynamic efficiency of a conventional airfoil.

2.5 CFD Simulation Setup

The FASIP(Flow-Acoustics-Structure Interaction Package) CFD code is used to conduct the numerical simulation. The 3D Reynolds Averaged Navier-Stokes (RANS) equations with one-equation Spalart-Allmaras(SA) turbulence model is used. A 5th order WENO scheme for the inviscid flux [26, 27, 28, 29, 30, 31] and a 2nd order central differencing for the viscous terms [26, 30] are employed to discretize the Navier-Stokes equations. The low diffusion E-CUSP scheme used as the approximate Riemann solver suggested by Zha et al [27] is utilized with the WENO scheme to evaluate the inviscid fluxes. Implicit time marching method using Gauss-Seidel line relaxation is used to achieve a fast convergence rate [32]. Parallel computing is implemented to save wall clock simulation time [33].

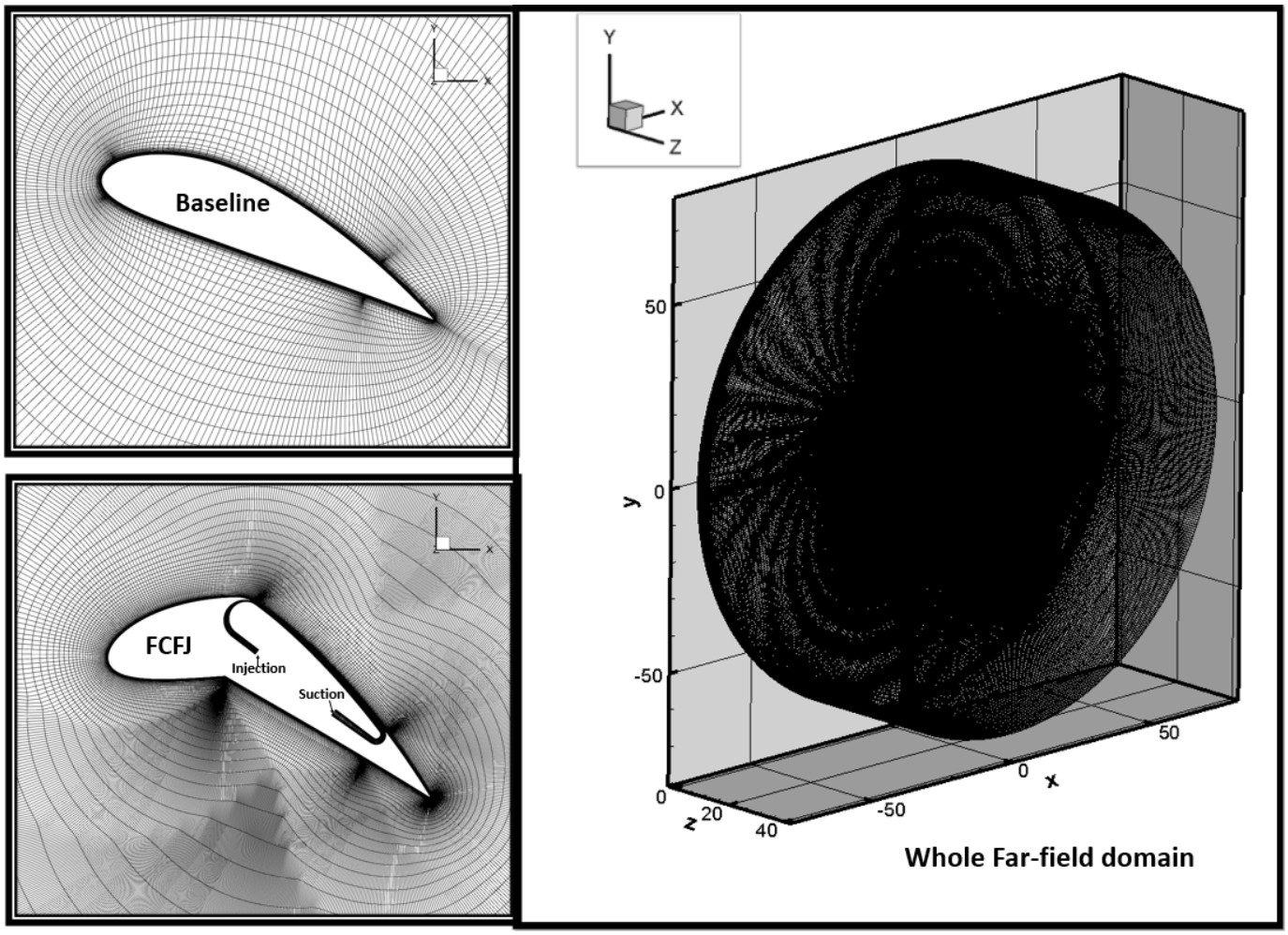

Figure 3: Computational mesh used in the current work.

2.6 Boundary Conditions

In order to achieve the flux conservation on the wall, the wall treatment provided in [34] imposes the 3rd-order accuracy no-slip condition on the solid surface. The far-field boundary is located at 55 chord with a O-mesh topology. The computational mesh is shown in Fig. 3 with a total mesh size of 2.5M for the baseline wing and 7.9M for the CFJ wing. Total pressure, total temperature and flow angles are specified at the upstream portion of the far field. Constant static pressure is applied at the downstream portion of the far field. The first grid point on the wing surface is placed at $y^+ \approx 1$.

3 Airfoil Geometry Parameters

Table 1 presents the detailed parameters of airfoils based on the NACA6421 standard, where injection and suction slot sizes are normalized by the airfoil chord length (C). The flapped CFJ6421-SST150-SUC133 (FCFJ) airfoil is developed based on the NACA 6421 airfoil, sharing the same suction surface translation (SST) of 1.50%C and suction slot size of 1.33%C as the regular CFJ. In the 2D FCFJ study[23], the optimal deflection(β) is 35° to

40° with an injection slot size of 0.4%C for a cruise condition, while keeping the suction slot size fixed at 1.33%C. To compare with the baseline experimental values, a validation analysis is performed at an aspect ratio of 6. In the case of FCFJ wings, studies are conducted at aspect ratios of 6, 10, and 20.

Table 1: Airfoil geometry parameters

Airfoil	Deflection Angle (β)	SST(%C)	INJ(%C)	SUC(%C)	AR
NACA6421 Baseline	N/A	N/A	N/A	N/A	6
Flapped CFJ(FCFJ)	35°, 40°	1.5	0.4	1.33	6, 10, 20

4 Results and Discussion

4.1 Baseline Validation

To validate the experimental result of the NACA6421 airfoil[35] with the FASIP CFD code, the coefficient of lift, drag, and aerodynamic efficiency C_L/C_D, according to the angle of attack(AoA) was examined. To match the experimental conditions, calculations were performed in the range of AoA -8° to 30° under the conditions of aspect ratio of 6, Re is 3.0×10^6, and Mach number of 0.065. Comparing the results, it is confirmed that the lift coefficient C_L, drag coefficient C_D, and C_L/C_D are all in good agreement with the experimental results under the stall AoA of 16 ° as shown in Fig 4 and 5. In AoA after Stall, the C_L shows a slightly higher value of 5-8% compared to the experimental value, but the C_D and C_L/C_D are predicted very well. Overall, this validation shows that the CFD solver, mesh and boundary conditions setup can perform this study well.

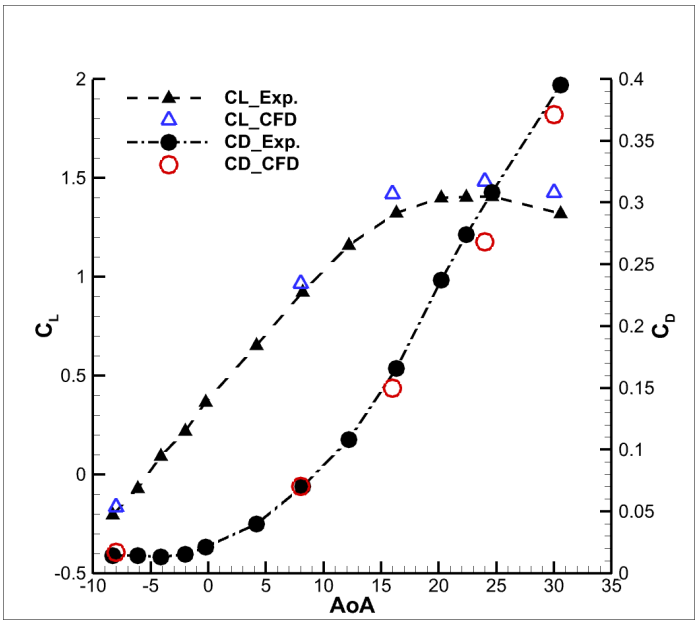

Figure 4: Lift and Drag coefficient for NACA6421 baseline

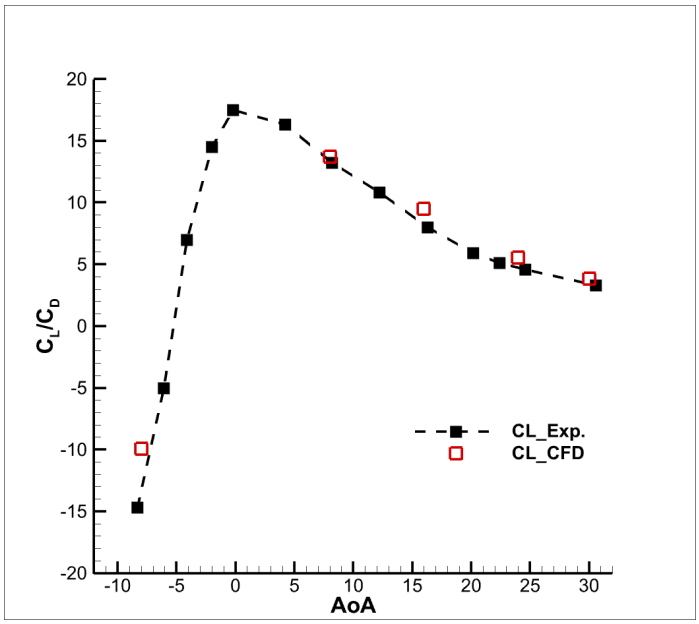

Figure 5: Aerodynamic efficiency for NACA6421 baseline

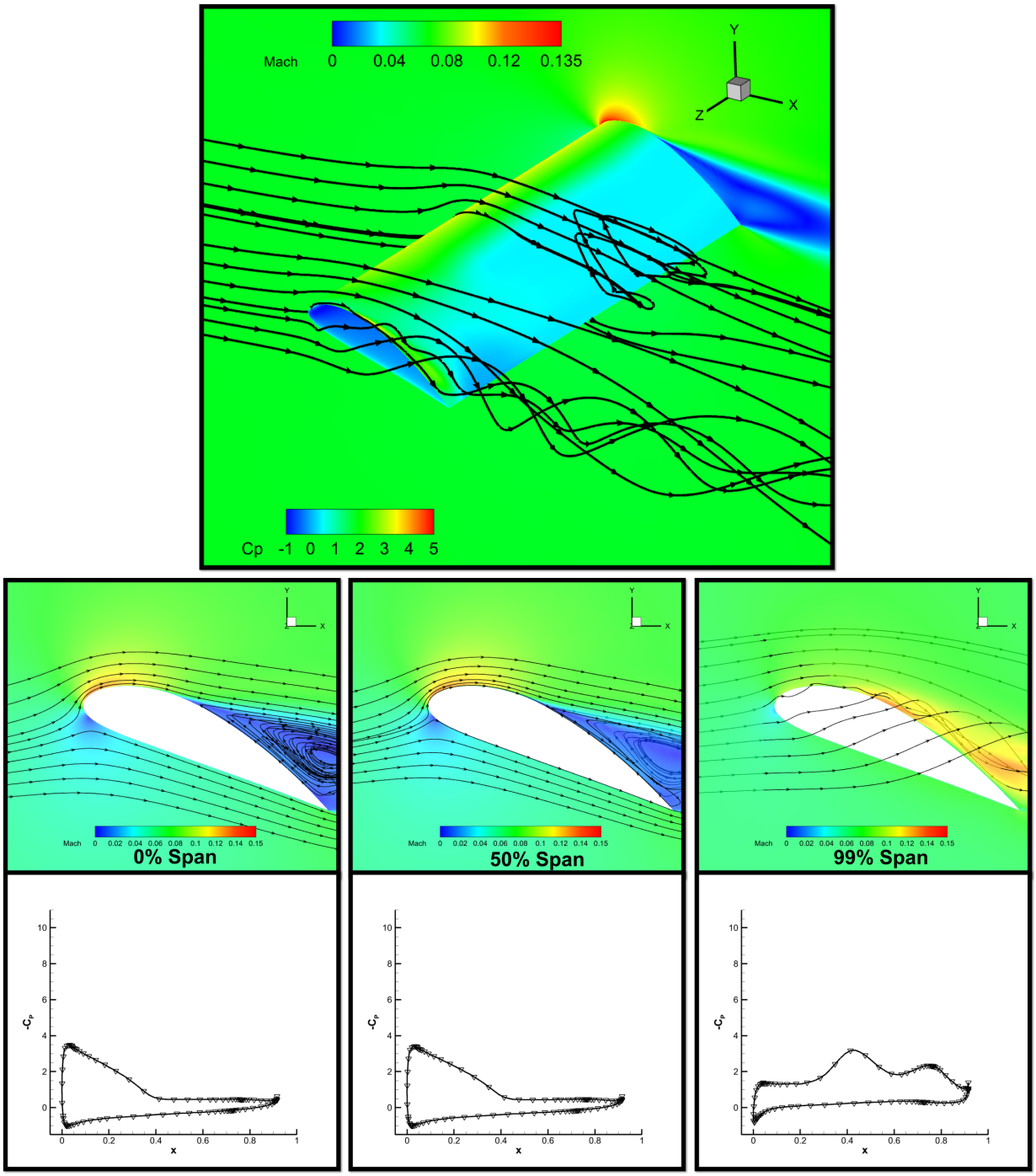

Figure 6: NACA6421 Baseline wing flow field and pressure coefficient at AoA of 24°

Fig.6 shows the flow field and C_p distribution at AoA 24°. As shown in Fig.4, a maximum C_L of 1.48 is obtained at this angle, but the C_D is high due to the separation, resulting in a C_L/C_D of 5.5. Near the leading edge, $-C_p$ has a maximum value with the highest flow velocity. The $-C_p$ value gradually decreases and the $-C_p$ value is very low due to the separation, and the drag increases beyond about 40%/C. Near the tip, the C_p distribution is not typical due to the vortex and the drag is very high.

4.2 Results for FCFJ Wings

For this study, the Reynolds number Re is 3.48×10^6 and the Mach number is 0.17 to match a potential cruise mission. The injection jet momentum coefficient C_μ of 0.06 and 0.11 is used for a trade study. The study begins with an aspect ratio of 6 that matches the baseline non-controlled wing. An aspect ratio of 20 is simulated after. The 2D optimal FCFJ airfoil obtained in [23] that is described in Section 3 is adopted to form the 3D finite wing.

The AoA is 23.5 degrees when the β is 35. As depicted in Fig. 4 for the baseline, the lift coefficient start decreasing at this angle while the drag coefficient climbs quickly since the baseline wing flow is largely separated. The FCFJ wing with AR of 6 does not have flow separation as shown in the flow field of Fig. 7 with a lift coefficient of 3.1 and C_μ of 0.1. The C_p distribution has a distinct shape from the baseline, with a very high peak at the shoulder of the flap that the injection is located. The C_p value of the FCFJ wing at the leading edge is abut the same as that of the baseline as shown in Fig. 6, but it continues to rise to the peak at the flap shoulder, resulting in a substantially increased lift coefficient compared to the baseline. The C_L/C_D is 5.63 and the corrected aerodynamic efficiency is 4.87, not very high due to the low AR of 6 and the strong tip vortex effect that generates a high induced drag. The Mach contours near the tip of the FCFJ wing shows a strong tip vortex. Fig.8 shows the results for AR of 20 and shows a similar C_p distribution to AR of 6. Similarly, the tip vortex effect occurs, but with a higher aspect ratio, the C_L is increased by about 21% compared to AR of 6 to 3.76, the C_D is halved to 0.27, and $(C_L/C_D)c$ of 10.55 is obtained at C_μ of 0.1. In this study, the CFJ is applied along the full span from the root to the tip. According to the 3D wing study of Lei et al [36], applying CFJ within 10% span near the tip has little benefit other than consuming the energy for CFJ. Future study will investigate the tip region effectiveness using CFJ.

Fig. 9 displays the effect of varying C_μ on the lift and drag coefficients for the FCFJ wing at AR of 20, while Fig. 10 presents the power coefficient and corrected aerodynamic efficiency. Fig. 9 shows that as C_μ increases the lift coefficient increases as well as the, the energy required by CFJ. However, it is important to note that the behavior of the drag coefficient with increasing C_μ differs between 2D and 3D configurations. In 2D, the drag coefficient tends to decrease with increasing C_μ due to reduced pressure drag. While in 3D, the opposite occurs because the induced drag grows with the lift coefficient, resulting in a stronger pressure drag force. Therefore, as C_μ increases, both the lift and drag coefficients tend to increase, with the pressure drag coefficient being higher when β is 40°. It should be noted that the increase in C_μ is directly proportional to the power consumption required for CFJ. Moreover, at β of 35°, variation of $(C_L/C_D)c$ with $C\mu$ from 0.06 to 0.1 is less than 10%, indicating that the impact of varying C_μ on the wing's overall efficiency is relatively small in this range. For the FCFJ configuration studied in this paper, the deflection angle of 35° provides the optimal overall performance that includes the high cruise C_L and $(C_L/C_D)_c$.

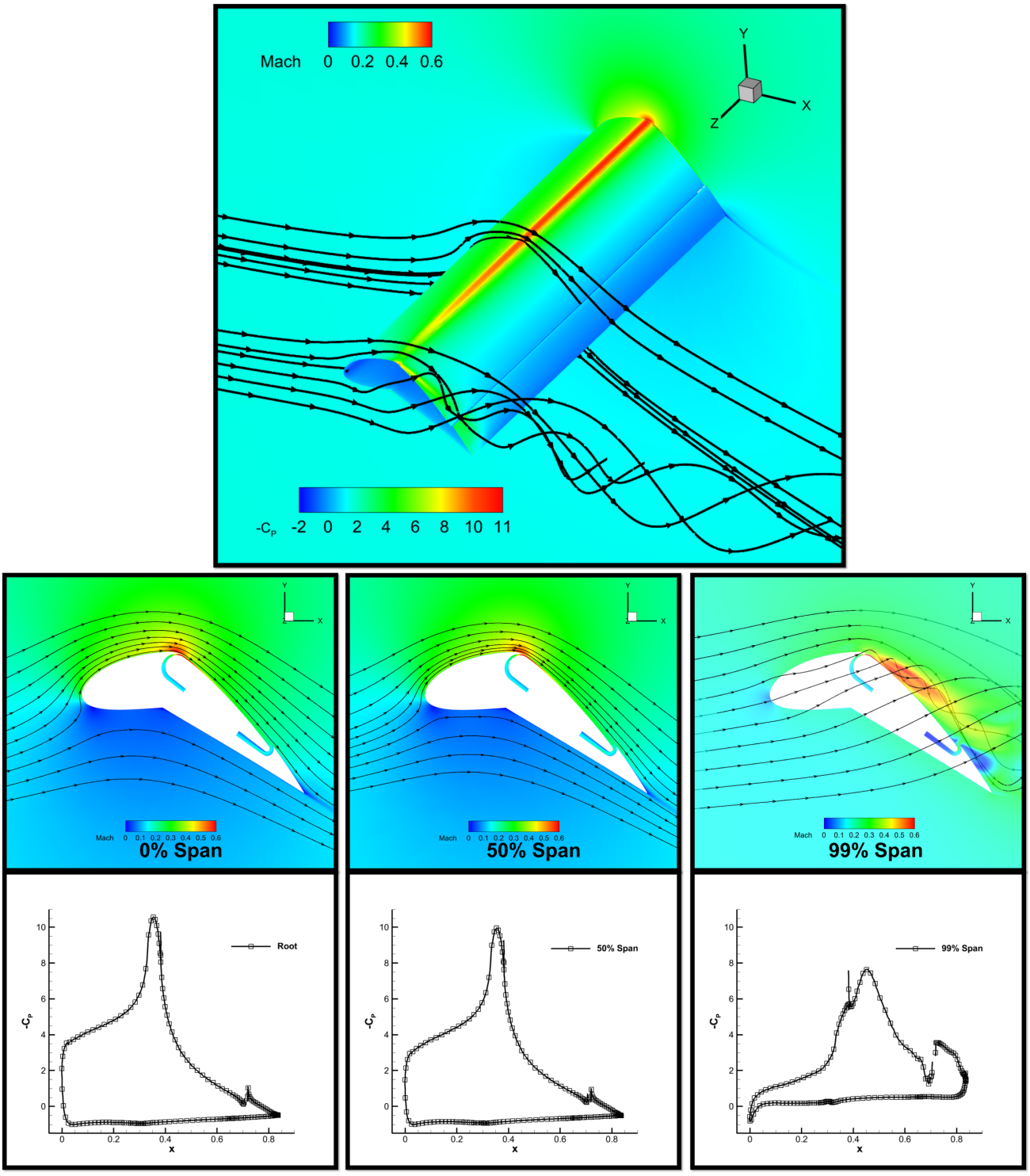

Figure 7: FCFJ flow field and pressure coefficient at flap deflection angle of 35° with AR6

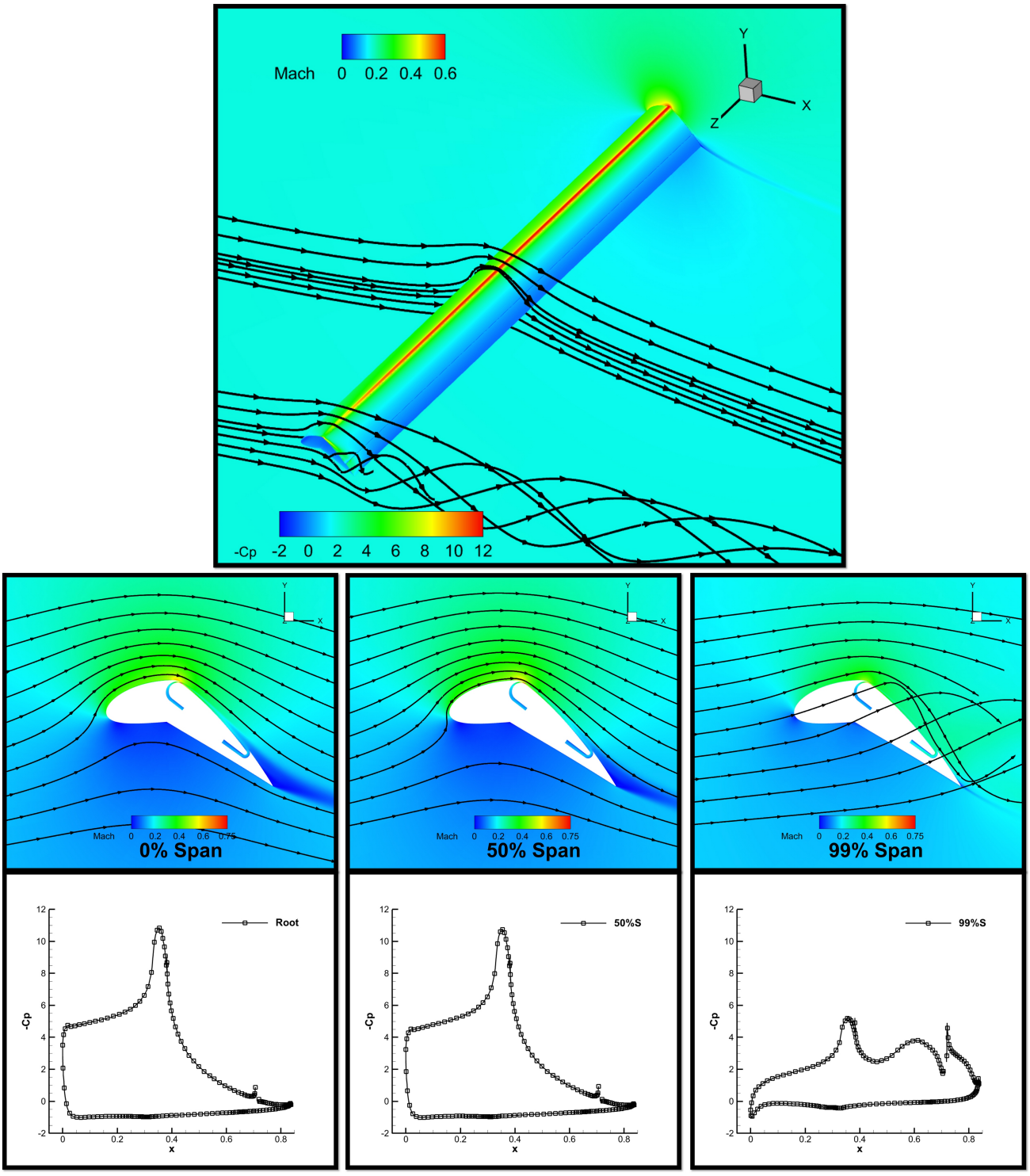

Figure 8: FCFJ flow field and pressure coefficient at flap deflection angle of 35° with AR20

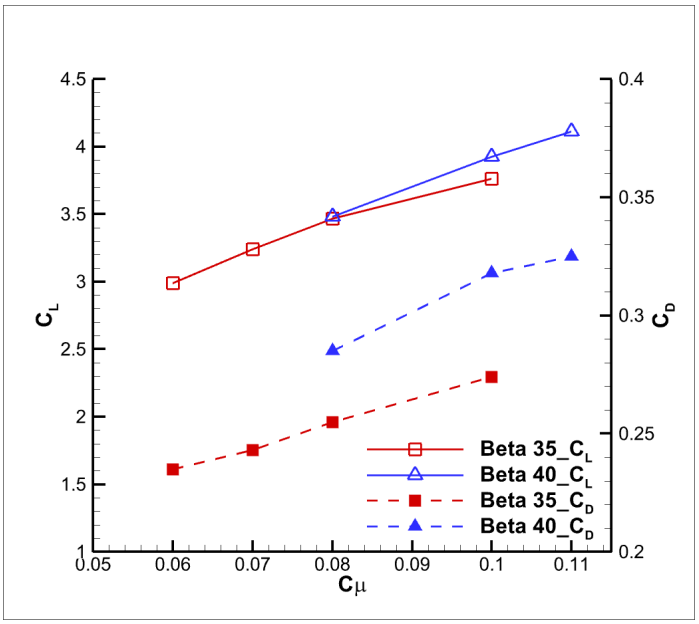

Figure 9: Lift and Drag coefficient for 3D FCFJ with AR20

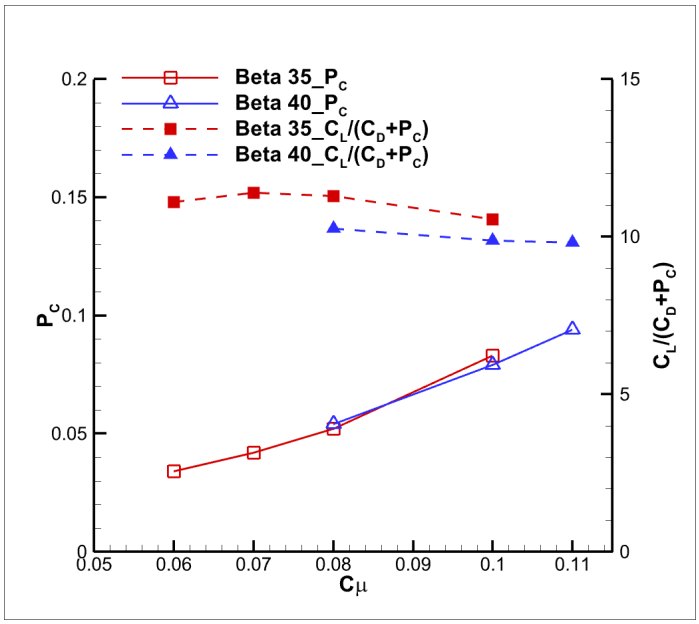

Figure 10: Aerodynamic efficiency for 3D FCFJ with AR20

Table 2 summarizes the results of the 3D analysis shown in Fig. 9 and Fig. 10 . At the high AR of 20, increased the C_L and $(C_L/C_D)_c$ obtained close to the target high cruise C_L and acceptable $(C_L/C_D)_c$ are 3.76 and 10.55, respectively with the deflection angle of 35° and the C_μ of 0.1. At β of 40°, the FCFJ wing with AR of 20 and C_μ of 0.1 has a slightly higher C_L and a more than 10% higher C_D, which results in a lower $(C_L/C_D)_c$ of 9.87. Same as the 2D study [23], the deflection angle of 35° provides the optimal overall performance.

Table 2: Aerodynamic performance for 3D FCFJ airfoils

AR	β	AoA	C_μ	C_L	C_D	C_L/C_D	C_M	P_c	$(C_L/C_D)_c$
6	35	23.5	0.1	3.098	0.550	5.63	-0.272	0.086	4.87
10	35	23.5	0.1	3.438	0.421	8.16	-0.260	0.083	6.82
20	35	23.5	0.06	2.991	0.235	12.70	-0.185	0.034	11.10
20	35	23.5	0.07	3.241	0.243	13.33	-0.199	0.042	11.39
20	35	23.5	0.08	3.466	0.255	13.59	-0.217	0.052	11.28
20	35	23.5	0.1	3.764	0.274	13.74	-0.250	0.083	10.55
20	40	27	0.08	3.480	0.285	12.20	-0.187	0.054	10.25
20	40	27	0.1	3.922	0.318	12.32	-0.221	0.079	9.87
20	40	27	0.11	4.110	0.325	12.65	-0.233	0.094	9.81

5 Conclusions

This paper studies 3D wings formed by Coflow jet flapped airfoil in order to achieve a cruise lift coefficient about one order of magnitude greater than that of conventional wing with a reasonable aerodynamic efficiency.

A high cruise lift coefficient is important for ultra-high altitude flight on Earth and flight in Martian atmosphere to overcome the low atmospheric density. The research employs a 3D RANS solver with Spalart-Allmaras(SA) turbulence model, a fifth-order WENO scheme for the inviscid fluxes, second-order central differencing for the viscous terms. As a validation, the numerical simulation achieves a very good agreement with the experiment for a 3D wing formed by NACA6421 airfoil with an aspect ratio of 6. The study investigates the 3D CFJ flapped wing at aspect ratio(AR) of 6, 10 and 20 at a freestream Mach number of 0.17 and Reynolds number of 3.48×10^6. For the one with AR of 20, a C_L of 3.76 and a moderate $(C_L/C_D)_c$ of 10.55 are obtained. This research indicates that cruise flight at an ultra-high lift coefficient with an acceptable aerodynamic efficiency appears to be feasible.

6 Acknowledgment

Disclosure: The University of Miami and Dr. Gecheng Zha may receive royalties for future commercialization of the intellectual property used in this study. The University of Miami is also equity owner in CoFlow Jet, LLC, licensee of the intellectual property used in this study.

References

[1] G.-C. Zha and D. C. Paxton, "A Novel Flow Control Method for Airfoil Performance Enhancement Using Co-Flow Jet." *Applications of Circulation Control Technologies*, Chapter 10, p. 293-314, Vol. 214, Progress in Astronautics and Aeronautics, AIAA Book Series, Editors: Joslin, R. D. and Jones, G.S., 2006.

[2] G.-C. Zha, W. Gao, and C. Paxton, "Jet Effects on Co-Flow Jet Airfoil Performance," *AIAA Journal, No. 6,*, vol. 45, pp. 1222–1231, 2007.

[3] G.-C. Zha, C. Paxton, A. Conley, A. Wells, and B. Carroll, "Effect of Injection Slot Size on High Performance Co-Flow Jet Airfoil," *AIAA Journal of Aircraft*, vol. 43, 2006.

[4] G.-C. Zha, B. Carroll, C. Paxton, A. Conley, and A. Wells, "High Performance Airfoil with Co-Flow Jet Flow Control," *AIAA Journal*, vol. 45, 2007.

[5] Wang, B.-Y. and Haddoukessouni, B. and Levy, J. and Zha, G.-C., "Numerical Investigations of Injection Slot Size Effect on the Performance of Co-Flow Jet Airfoil," *Journal of Aircraft*, vol. Vol. 45, No. 6,, pp. pp.2084–2091, 2008.

[6] B. P. E. Dano, D. Kirk, and G.-C. Zha, "Experimental Investigation of Jet Mixing Mechanism of Co- Flow Jet Airfoil." AIAA-2010-4421, 5th AIAA Flow Control Conference, Chicago, IL, 28 Jun - 1 Jul 2010.

[7] B. P. E. Dano, G.-C. Zha, and M. Castillo, "Experimental Study of Co-Flow Jet Airfoil Performance Enhancement Using Micro Discreet Jets." AIAA Paper 2011-0941, 49th AIAA Aerospace Sciences Meeting, Orlando, FL, 4-7 January 2011.

[8] A. Lefebvre, B. Dano, W. Bartow, M. Fronzo, and G. Zha, "Performance and energy expenditure of coflow jet airfoil with variation of mach number," *Journal of Aircraft*, vol. 53, no. 6, pp. 1757–1767, 2016.

[9] A. Lefebvre, G-C. Zha, "Numerical Simulation of Pitching Airfoil Performance Enhancement Using Co-Flow Jet Flow Control," *AIAA paper 2013-2517*, June 2013.

[10] A. Lefebvre, G-C. Zha, "Cow-Flow Jet Airfoil Trade Study Part I : Energy Consumption and Aerodynamic Performance," *Proceedings of the AIAA Flow Control Conference*, June 2014.

[11] A. Lefebvre, G-C. Zha, "Cow-Flow Jet Airfoil Trade Study Part II : Moment and Drag," *Proceedings of the AIAA Flow Control Conference*, June 2014.

[12] Yunchao Yang, Gecheng Zha, "Super-Lift Coefficient of Active Flow Control Airfoil: What is the Limit?," *AIAA Paper 2017-1693, AIAA SCITECH2017, 55th AIAA Aerospace Science Meeting, Grapevine, Texas, 9-13 January 2017*, 2017.

[13] Gecheng Zha, Yunchao Yang, Yan Ren, Brendan McBreen, "Super-Lift and Thrusting Airfoil of Coflow Jet Actuated by Micro-Compressors," *AIAA Paper-2018-3061, AIAA AVIATION Forum 2018, Flow Control Conference, June 25-29*, 2018.

[14] Lefebvre, A. and Zha, G.-C., "Trade Study of 3D Co-Flow Jet Wing for Cruise Performance." AIAA Paper 2016-0570, AIAA SCITECH2016, AIAA Aerospace Science Meeting, San Diego, CA, 4-8 January 2016.

[15] Kewei Xu, Gecheng Zha, "High Control Authority 3D Aircraft Control Surfaces Using Co-Flow Jet," *AIAA Journal of Aircraft*, 2020.

[16] Kewei Xu, Yan Ren, Gecheng Zha, "Numerical Analysis of Energy Expenditure for Co-Flow Wall Jet Separation Control," *AIAA Journal, published online: 11 Jan 2022, doi.org/10.2514/1.J061015*, 2022.

[17] Lefebvre, A. and Zha, G.-C. , "Design of High Wing Loading Compact Electric Airplane Utilizing Co-Flow Jet Flow Control." AIAA Paper 2015-0772, AIAA SciTech2015: 53nd Aerospace Sciences Meeting, Kissimmee, FL, 5-9 Jan 2015.

[18] Yang Wang and Gecheng Zha, "Study of Mach Number Effect for 2D Co-Flow Jet Airfoil at Cruise Conditions," *AIAA Paper 2019-3169, AIAA Aviation 2019 Forum, 17-21 June 2019, Dallas, Texas*, 2019.

[19] Yang Wang and Gecheng Zha, "Study of Mach Number Effect for 3D Co-Flow Jet Wings at Cruise Conditions," *AIAA Paper 2020-0045, AIAA SciTech Forum, 6-10 January 2020, Orlando, FL*, 2020.

[20] Yan Ren, Gecheng Zha, "Performance Enhancement by Tandem Wings Interaction of CoFlow Jet Aircraft," *AIAA Paper 2021-1823, AIAA SciTech Forum, 11–15; 19–21 January 2021, VIRTUAL EVENT*, 2021.

[21] Paula A. Barrios, Yan Ren, GeCheng Zha, "Simulation of 3D Co-Flow Jet Airfoil Control with Micro-Compressor Actuator at High Angles of Attack," *Proceedings of AIAA Aviation Forum 2023, 12–16 June 2023, San Diego, CA*, 2023.

[22] Yang Wang, Yunchao Yang and Gecheng Zha, "Study of Super-Lift Coefficient of Co-Flow Jet Airfoil and Its Power Consumption," *AIAA Paper 2019-3652, AIAA Aviation 2019 Forum, 17-21 June 2019, Dallas, Texas* , 2019.

[23] Jaehyoung Jeon, Yan Ren, and Gecheng Zha, "Toward Ultra-High Cruise Lift Coefficient Using Flapped CoFlow Jet Airfoil," *Pending, AIAA Paper 2023, AIAA SciTech Forum, January 23-27*, 2023.

[24] Zha, G.-C,, "Feasibility Study of Deflected Slipstream Airfoil for VTOL Hover Enabled by CoFlow Jet," *Proceedings of AIAA Aviation Forum 2023, 12–16 June 2023, San Diego, CA*, 2023.

[25] Kewei Xu, Yan Ren, and Gecheng Zha, "Separation Control by Co-Flow Wall Jet," *AIAA Paper 2021-2946, AIAA AVIATION Forum, August 2-6*, 2021.

[26] Y.-Q. Shen and G.-C. Zha, "Large Eddy Simulation Using a New Set of Sixth Order Schemes for Compressible Viscous Terms ," *Journal of Computational Physics*, vol. 229, pp. 8296–8312, 2010.

[27] Zha, G.C., Shen, Y.Q. and Wang, B.Y., "An improved low diffusion E-CUSP upwind scheme ," *Journal of Computer and Fluids*, vol. 48, pp. 214–220, Sep. 2011.

[28] Y.-Q. Shen and G.-Z. Zha , "Generalized finite compact difference scheme for shock/complex flowfield interaction," *Journal of Computational Physics*, vol. doi:10.1016/j.jcp.2011.01.039, 2011.

[29] Shen, Y.-Q. and Zha, G.-C. and Wang, B.-Y., " Improvement of Stability and Accuracy of Implicit WENO Scheme," *AIAA Journal*, vol. 47, No. 2, pp. 331–344, 2009.

[30] Shen, Y.-Q. and Zha, G.-C. and Chen, X.-Y., " High Order Conservative Differencing for Viscous Terms and the Application to Vortex-Induced Vibration Flows," *Journal of Computational Physics*, vol. 228(2), pp. 8283–8300, 2009.

[31] Shen, Y.-Q. and Zha, G.-C. , " Improvement of the WENO Scheme Smoothness Estimator," *International Journal for Numerical Methods in Fluids*, vol. DOI:10.1002/fld.2186, 2009.

[32] G.-C. Zha and E. Bilgen, "Numerical Study of Three-Dimensional Transonic Flows Using Unfactored Upwind-Relaxation Sweeping Algorithm," *Journal of Computational Physics*, vol. 125, pp. 425–433, 1996.

[33] B.-Y. Wang and G.-C. Zha, "A General Sub-Domain Boundary Mapping Procedure For Structured Grid CFD Parallel Computation," *AIAA Journal of Aerospace Computing, Information, and Communication*, vol. 5, No.11, pp. 2084–2091, 2008.

[34] Y.-Q. Shen, G.-C. Zha, B.-Y. Wang, "Improvement of stability and accuracy of implicit WENO scheme," *AIAA Journal*, vol. 47, pp. 331–344, 2009.

[35] EASTMAN N.JACOBS, KENNETH E. WARD, and ROBERT M.PINKERTON, "THE CHARACTERISTICS OF 78 RELATED AIRFOIL SECTIONS FROM TESTS IN THE VARIABLE-DENSITY WIND TUNNEL," *REPORT No.460*, 1935.

[36] Zjijin Lei, Gecheng Zha, "Numerical Study of Co-Flow-Jet Distribution along the Span of Finite Wing," *AIAA Paper-2023-2609, AIAA SCITECH 2023 Forum, 23-27 January 2023, National Harbor, MD*, 2023.